ECCOMAS Thematic Conference on Computational Methods
in Structural Dynamics and Earthquake Engineering
M. Papadrakakis, D.C. Charmpis, N.D. Lagaros, Y. Tsompanakis (eds.)
Rethymno, Crete, Greece, 13–16 June 2007

MODELLING INELASTIC BUCKLING OF REINFORCING BARS UNDER EARTHQUAKE LOADING

Michalis Fragiadakis[1*], Rui Pinho[2], Stelios Antoniou[3]

[1] School of Civil Engineering, National Technical University of Athens,
Zografou Campus, Athens 157 80, Greece
mfrag@mail.ntua.gr

[2] European School for Advanced Studies in Reduction of Seismic Risk (ROSE School)
c/o EUCENTRE, Via Ferrata 1, 27100 Pavia, Italy
rui.pinho@eucentre.it

[3] Seismosoft, 21 Perikleous Stavrou Str., Chalkis 34100, Greece
s.antoniou@seismosoft.com

Keywords: Buckling of steel bars, Monti-Nuti model, Menegotto-Pinto model, nonlinear timehistory analysis.

Abstract. *This study focuses on the modelling of steel reinforcing bars subjected to a generalized loading history. The model of Monti and Nuti which is based on a set of experimental observations in order to account for buckling of the steel bars is examined. It has been noticed that in the case of partial unloading and then reloading, a common situation when a structure is subjected to seismic actions, the model might greatly overestimate the corresponding stress. An additional memory rule is thus proposed to eliminate this observed shortcoming. With the aid of the proposed modification, the Monti-Nuti model proved to be capable of simulating accurately the capacity of reinforced concrete members. The rules presented are easy to implement and applicable to any model in the literature where a similar situation is identified. Two case studies are examined where the enhanced model was proven capable to produce realistic numerical results.*

1 INTRODUCTION

Past earthquakes have shown that a common failure mode of reinforced concrete (RC) members is buckling of the longitudinal reinforcement. In order to obtain an accurate prediction of strength and ductility, this effect should thus be taken into account during analysis. Buckling of the reinforcement is in essence a stability problem and therefore depends both on the geometry of the bar and on the material properties. However, treating the problem as a second-order problem would require a detailed FE modelling approach. In practice, in order to allow for an easier modelling of RC structures, phenomenological constitutive laws where buckling is taken into consideration through the material properties are commonly adopted.

The interest of this study is on uniaxial stress-strain relationships, which can be used in the framework of a fiber beam-column element and also can capture accurately the response of a linear element with minor bending stiffness such as a reinforcing bar. In particular, special attention is paid on the model proposed by Monti and Nuti [1]. This model incorporates a set of experimental observations regarding the response of steel reinforcement into the widely-used stress-strain relationship of Menegotto and Pinto [2].

Experience has shown that a stress-strain relationship may fail to predict correctly the response when small reversals in the strain history occur; this is the case when the structural model is subjected to a ground motion record. Initially this problem was identified in the model of Menegotto and Pinto [2] by Filippou *et al.* [3], who pointed out that, in order to avoid such an undesirable behaviour, the memory of the analytical model should extent over all previous branches of the stress-strain history. In terms of implementation this would be impractical and thus Filippou *et al.* [3] proposed to limit the memory of the model to four controlling curves, which warrant that, at least at the structural level, this numerical problem is almost fully eliminated.

The aforementioned numerical difficulty strongly manifests itself when the Monti-Nuti buckling rules [1] are implemented on the model of Menegotto and Pinto [2], even if the Filippou *et al.* [3] modifications are adopted; the response may be heavily distorted, thus limiting the applicability of the model to non-earthquake engineering applications. In this work, an additional memory rule that enables more accurate handling of a generalized load history is proposed. The methodology proposed is general in scope since it can be applied almost to any constitutive law of a $\sigma = f(\varepsilon)$ type, including the Menegotto-Pinto and the Monti-Nuti models. Emphasis is placed on the Monti-Nuti relationship, where the problem is more critical and also because the Menegoto-Pinto model does not feature modelling of re-bar buckling.

2 GENERAL SPECIFICATIONS

2.1 Description of the physical problem

During load reversals, concrete in compression zone prevents the development of high compressive strain in the compressive steel. Only when concrete loses its resistance, as in the case of concrete spalling, the development of high compressive strain in reinforcing steel is likely. After spalling of the concrete cover the longitudinal bars are exposed and if the amplitude of the cyclic loading is significant the bars will buckle outwards. The only factor contributing against buckling is the existence of stirrups, that should be sufficiently spaced and detailed, particularly in those parts of the member where heavy inelasticity excursion is likely to take place.

Several parameters are involved in the phenomenon of buckling such as the slenderness of the rebar, the stiffness and the rigidity of the hoops and the strain hardening of steel. The most important is probably the slenderness of the rebars. A measure of slenderness is given by the

ratio between the length of the stirrups over the diameter of the bar, L/D. The failure modes usually observed are, primarily, buckling between two consecutive stirrups and, less commonly, along a larger length when fracture of more than one stirrup occurs.

Only the monotonic behaviour has been thoroughly investigated when it comes to buckling, while the cyclic behaviour is still under investigation. According to Mander *et al.* [4] buckling takes place at or near the yielding load, which is also verified by the recent study of Bae *et al.* [5]. The monotonic post-buckling path varies for different slenderness ratios of the bar. Mau and El-Mabsout [6] presented monotonic curves for different, L/D ratios, where it is concluded that the higher the values of the ratio L/D, the lower the post-buckling peak stress. They have also verified numerically that the transition point between elements that are subjected to buckling phenomena and those that are not, is for L/D values close to five. For ratio values smaller than this threshold, the stress-strain relationship remains similar to that in tension. Monti and Nuti [1] and Cosenza and Prota [7] both presented results where the above threshold was justified experimentally, while Bae *et al.* [5] concluded, on the basis of extended experiments, that this threshold value may vary also according to the yield strength of the bar. Moreover, Cosenza and Prota [7] showed that for L/D ratio values greater than 20, elastic buckling is more likely to occur.

2.2 State-of-the-art in modelling of the bars of steel bars

Few attempts to capture buckling of the longitudinal bars can be found in the literature. Among them, the proposals of Gomes and Appleton [8] and Monti and Nuti [1] are based on modifications of the Menegotto-Pinto model [2]. Monti and Nuti [1] proposed a set of rules based on experimental observations of buckling of reinforcement bars. The stress-strain relationship adopted was that of Menegotto-Pinto, though any given constitutive law may be used, if expressed accordingly. The parameters of the Monti-Nuti model are updated after each load reversal, with such updating being performed by means of the two classical (*i*) isotropic and (*ii*) kinematic hardening rules, (*iii*) a memory rule to account for the material's memory of the plastic path followed and (*iv*) a saturation rule to account for the asymptotic character of the hardening phenomena. These four rules are defined both in the absence and in the presence of buckling. A detailed description of the model is provided by Monti and Nuti [1], where experiment-based values are used in order to calibrate the model; different values can be easily adopted on the basis of alternative experiments (e.g. [5,7]). A brief description of the Monti-Nuti is given in the following paragraphs.

The backbone of the Monti-Nuti model is that of the Menegotto-Pinto relationship:

$$\sigma^* = b\varepsilon^* + \frac{(1-b)\varepsilon^*}{\left(1+\varepsilon^{*R}\right)^{\frac{1}{R}}} \tag{1}$$

where the normalised strain and stress are obtained by:

$$\varepsilon^* = \frac{\varepsilon - \varepsilon_r}{\varepsilon_0 - \varepsilon_r} \quad \text{and} \quad \sigma^* = \frac{\sigma - \sigma_r}{\sigma_0 - \sigma_r} \tag{2}$$

Eq. (1) represents a curved transition from a straight-line asymptote with slope E_0 to another asymptote with slope bE_0 (Fig. 1 lines (α) and (β) respectively). σ_0 and ε_0 are the stress and the strain at the point where two asymptotes of the branch under consideration meet (Fig. 1, point A), while σ_r and ε_r denote the stress and strain at the point where the last strain rever-

sal with stress of equal sign took place (Fig. 1, point B). The shape of the transition curve allows a good representation of the Baushinger effect. This is a function of the curvature parameter R and depends on the strain difference between the current asymptote intersection point and the previous load reversal point with maximum or minimum strain depending on the corresponding steel stress [3].

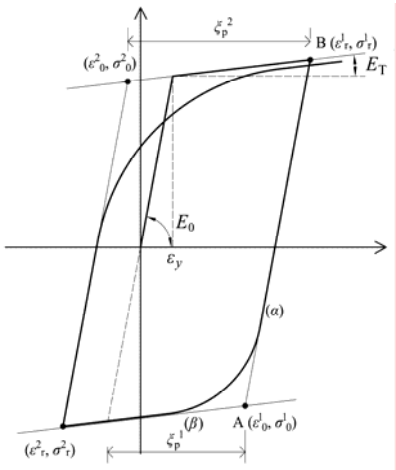

Fig. 1. Stress-strain relationship of the Menegotto-Pinto model

The expression for R takes the form: $R^n = R_0 - \left(a_1 \xi_p^n \Big/ \left(a_2 + \xi_p^n\right)\right)$, where ξ_p^n is the plastic excursion at the current semicycle, defined as: $\xi_p^n = \varepsilon_r^n - \varepsilon_y^n$. Also, R_0 is the value of the parameter R during the first loading and a_1, a_2 are experimentally determined parameters to be defined together with R_0. The hardening rules are functions of four independent parameters: yield stress σ_y, elastic modulus E_0, hardening ratio b_{0p} and a weighting coefficient P. In absence of buckling, experimental tests have shown that no isotropic hardening is developed in half-cycles with plastic excursion equal to or lower than the maximum previous one. In the presence of buckling a complementary phenomenon occurs, in this case no kinematic hardening is developed in half-cycles with plastic excursion equal to or lower than the maximum previous one. These phenomena are modelled through a memory rule based on the additional plastic excursion γ_p^n:

$$\gamma_p^n = \left\langle \left|\xi_p^n\right| - \xi_p^{\max} \right\rangle \cdot \operatorname{sign}\left\{\xi_p^n\right\} \tag{3}$$

where $\langle a \rangle = a$ if $a > 0$ and $\langle a \rangle = 0$ if and $\xi_p^{max} = max\left(\left|\xi_p^n\right|\right)$ is the maximum plastic excursion. The half-cycle plastic work is defined as:

$$\Phi_p^n = \frac{1}{2}\left(\sigma_r^n - \sigma_y^n\right) \xi_p^n \tag{4}$$

Φ_p^n in absence of buckling is positive both in tension and in compression, while in the presence of buckling it is positive in tension and negative in compression. The hardening ratio b_{0p} for post-yield hardening branches in tension is defined as the ratio between the post-yield modulus in tension and the initial elastic modulus. The curvature of the branch is defined as in the Menegotto-Pinto model. Some additional parameters are determined in order to account for buckling. The hardening ratio for post-yield softening branches in compression is defined as:

$$b_{0n} = 0.003\left(\left(L/D\right)^{*} - L/D\right) \tag{5}$$

which decreases with increasing L/D and is not related to the positive hardening ratio b_{0p}. In Eq. (5), $\left(L/D\right)^{*}$ denotes the threshold ratio beyond which inelastic buckling is expected to occur, usually taken equal to five. The curvature of the post-yield loading branches in compression follows the rule:

$$R_b = R_{0b} + \frac{a_{1b}\cdot\xi_p^{\max}}{a_{2b}+\xi_p^{\max}} < R_{1b} \tag{6}$$

where $R_{0b} = 0.2\left(L/D - \left(L/D\right)^{*}\right)$, $a_{1b} = a_1 + 1$, $a_{2b} = 1000a_2$, and $R_{1b} = R_0 - 2\left(L/D - \left(L/D\right)^{*}\right)$.

The elastic modulus after reversal from compression varies according to:

$$E = E_0\left(a_5 + \left(1-a_5\right)\cdot\exp\left(-a_6\xi_p^2\right)\right) \tag{7}$$

where $a_5 = 1 + \left(\left(L/D\right)^{*} - L/D\right)\Big/7.5$, and $a_6 = 1000$. The modulus decreases with increasing cycle amplitude, due to the bar axial stiffness degradation that takes place after buckling.

The total hardening is obtained by means of a mixed rule consisting of both a kinematic and an isotropic component. A linear combination of two of the hardening types is assumed using a weighing coefficient *P*, which is calibrated experimentally:

$$\Delta\sigma_{KI}^n = P\cdot\Delta\sigma_K^n + \left(1-P\right)\cdot\Delta\sigma_I^n\cdot\operatorname{sign}\left(-\xi_p^n\right) \tag{8}$$

A value of *P*=0.9 is suggested for common mild steel. The two hardening components are developed based on a memory rule. In the absence of buckling this rule is applied to the isotropic hardening, while in the presence of buckling it is applied to the kinematic hardening instead. In the absence of buckling the stress variation is due to the plastic excursion and the additional plastic excursion is given as follows:

Kinematic hardening:
$$\Delta\sigma_K^n = \sum_{i=1}^{n} b_{0n}\cdot E_0\cdot\xi_p^n \tag{9}$$

Isotropic hardening:
$$\Delta\sigma_I^n = \sum_{i=1}^{n}\left|b_{0n}\cdot E_0\cdot\gamma_p^n\right|\cdot\operatorname{sign}\left(\Phi_p^n\right) \tag{10}$$

On the contrary, in the presence of buckling the stress variation is due to the additional plastic excursion which is defined as:

Kinematic hardening:
$$\Delta\sigma_K^n = \sum_{i=1}^{n} b_{0n}\cdot E_0\cdot\gamma_p^n \tag{11}$$

Isotropic hardening:
$$\Delta\sigma_I^n = \sum_{i=1}^{n}\left|b_{0n}\cdot E_0\cdot\xi_p^n\right|\cdot\operatorname{sign}\left(\Phi_p^n\right) \tag{12}$$

The updated stress σ_0^n (or σ_y^{n+1}) of Eq. (1) becomes:

$$\sigma_y^{n+1} = \sigma_y^0\cdot\operatorname{sign}\left(-\xi_p^n\right) + \Delta\sigma_{KI}^n \tag{13}$$

3 RESPONSE UNDER A GENERALIZED LOAD HISTORY

When a ground motion is used to perform timehistory analysis, relatively small loading-unloading excursions of the material strains are frequent. Reinforcing bar numerical models, however, tend to be verified only under loading conditions such as that of Figure 2(a) where the loading scheme consists of large stable symmetric cycles. As a result, spurious numerical behaviour such as that illustrated in Fig. 2(b), that arise from random unsymmetrical loading cycles, might be overlooked.

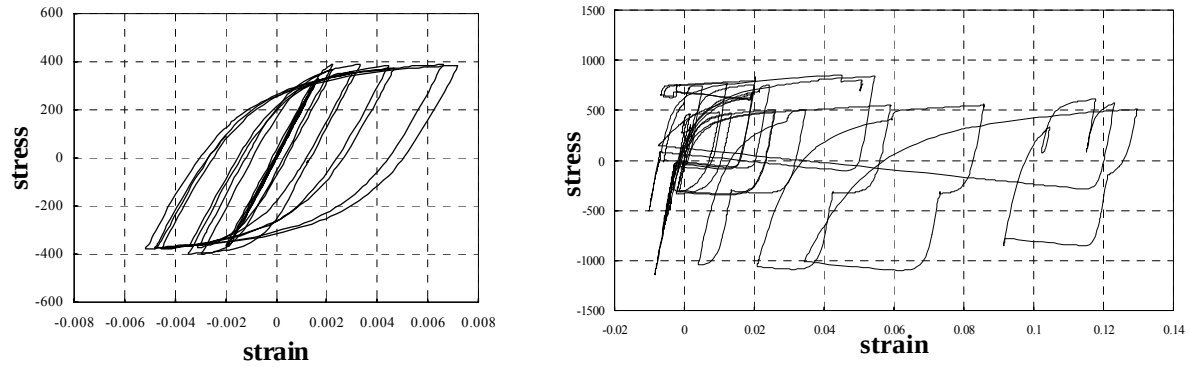

(a) (b)

Figure 2. (a) Response under stable cyclic strain history; (b) Spurious branches on the σ-ε level produced by the M-N model when the member is subjected to earthquake loading

The severity of the problem depends on the formulation of the material model used. In particular, the Monti-Nuti model was found to be very sensitive to this situation, since a tiny notch in the stress-strain path may lead to a very large overestimation of the corresponding stress (Fig. 2(b)). This is due to the fact that the bilinear envelope, defined by the Menegotto-Pinto model adopted by Monti and Nuti, becomes too narrow and the curves are not capable of "fitting" within it. Therefore, this spurious behaviour is generated because the same algebraic expression used for the skeleton curve is also used when a small unloading and loading back takes place. Consequently, the spurious branches of Fig. 2(b) are developed, with a shape that depends on the ratio between tie spacing and bar diameter L/D. As shown in sections to follow, such overestimations may affect the accuracy of the overall analysis, for which reason it was deemed necessary to address them accordingly, as discussed subsequently.

4 PROPOSED MODIFICATIONS

In order to tackle difficulties such as those discussed in the previous section, Dodd and Restrepo-Posada [9] introduced the idea of major, minor and simple reversals, whilst Balan and Filippou [10] distinguished reversals into complete and incomplete, with a value of $2f_y$ being adopted as a threshold parameter. For the Monti-Nuti model, Attolico *et al.*[11] proposed that whenever small strain variations take place, the model should follow the backbone curve before the last strain reversal.

In the current work, an alternative corrective measure is proposed for the Monti-Nuti model, where the stress-strain curve is forced to join tangentially the branch defined during the previous strain reversal. In order to determine whether an unloading branch is small or not, a strain interval denoted as $\hat{\varepsilon}$ is introduced. The latter is defined as a proportion of the strain value of the point of the last strain reversal ε_r. Typical efficient values vary between 2.5 or 5 percent of ε_r, though larger values may be used if higher "filtering" is deemed necessary [12].

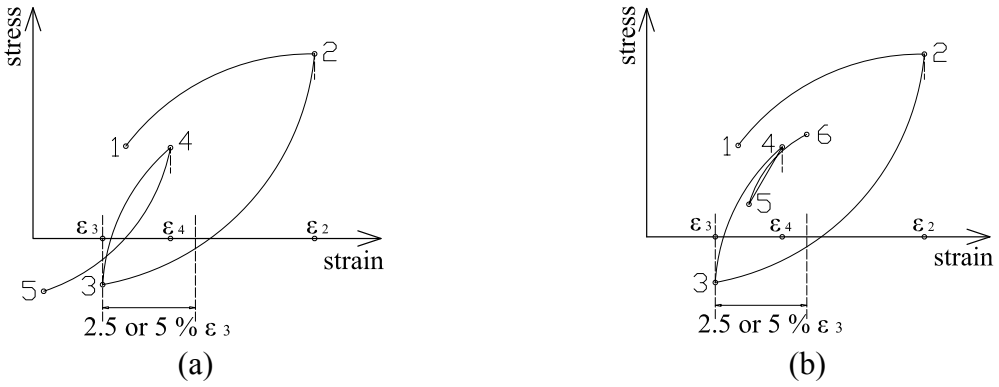

Figure 3. Reversal modelling in the $\hat{\varepsilon}$ interval

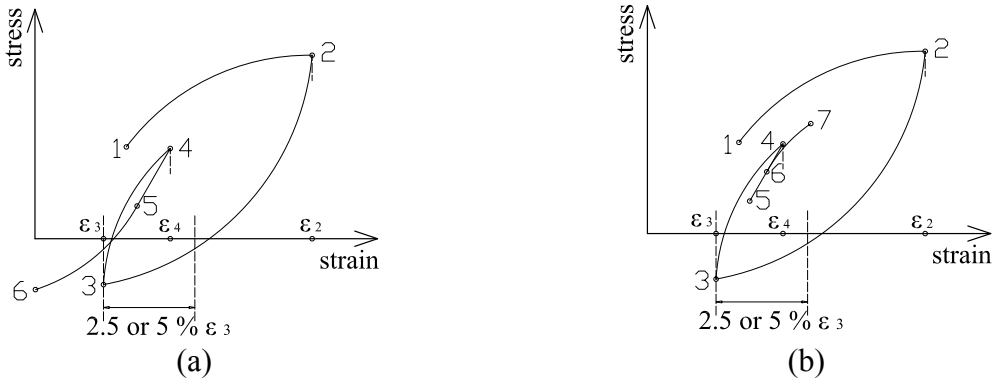

Figure 4. Reversal modelling in the $\hat{\varepsilon}$ interval, when reloading points obtained elastically.

All loading and reloading that takes place inside the interval $\hat{\varepsilon}$ are assumed to be linear elastic. Fig. 3(a) shows that when reloading beyond this interval (from point 4 to 5), the skeleton curve of the last loading branch is followed instead of updating the model parameters that would define a new loading branch. Otherwise, if unloading does not go beyond $\hat{\varepsilon}$, point 5 is obtained elastically (Fig. 3(b)). Loading in the opposite direction, beyond point 4, will follow the previously defined branch 3-4 (Fig. 3(b)). Fig. 4 shows two cases where reloading starts

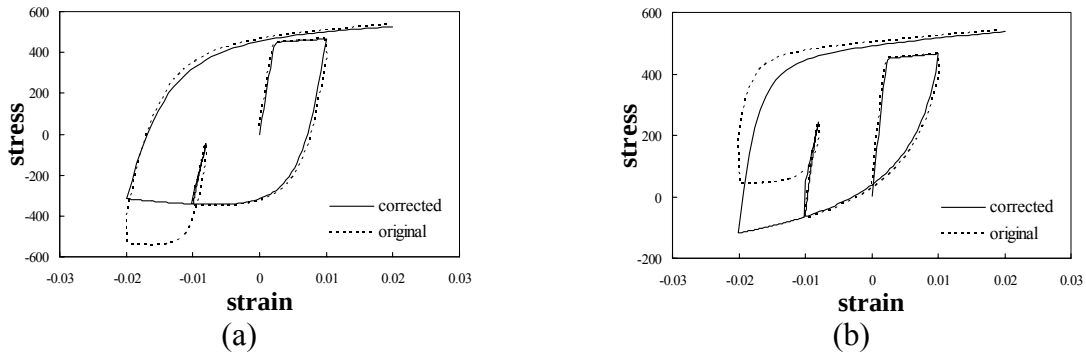

Figure 5. Corrected and uncorrected stress-strain paths; (a) L/D = 12, (b) L/D = 6.

from points that have been previously obtained elastically. A strain step that results in a strain value outside the $\hat{\varepsilon}$ interval will follow the previously defined skeleton branch curve (Fig. 4(*a*)). Fig. 4(*b*) shows that all load reversals inside $\hat{\varepsilon}$ are considered linear elastic. In Fig. 5,

the uncorrected and the corrected stress-strain histories for different L/D ratios are shown. Fig. 6 and Fig. 7, on the other hand, demonstrate the effectiveness of the algorithm at the stress-strain and the structural levels, respectively, when the structure is subjected to a ground motion record.

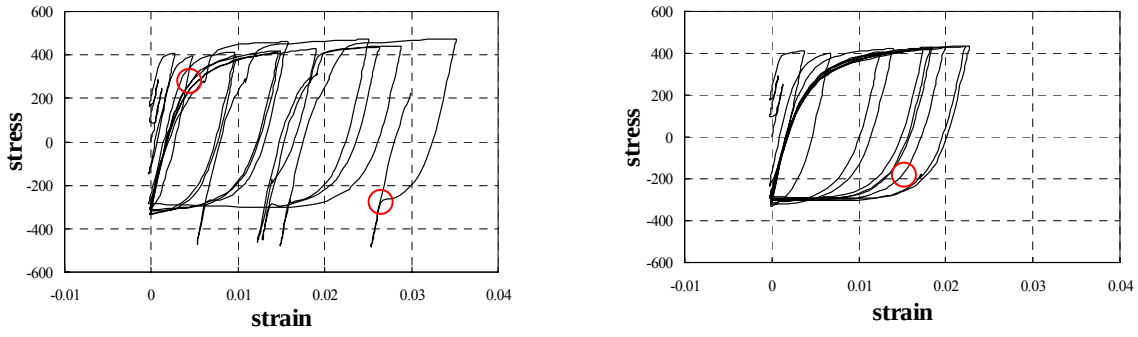

(a) (b)

Figure 6. Comparison at the stress-strain level under seismic excitation;
(a) without the proposed modifications, (b) with the proposed modifications.

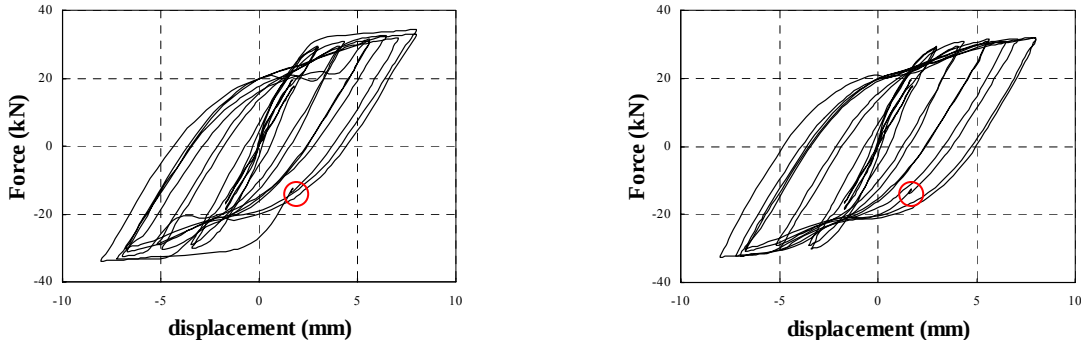

(a) (b)

Figure 7. Comparison at the structural level under seismic excitation;
(a) without the proposed modifications (b) with the proposed modifications.

5 CALIBRATION OF THE MODEL

The applicability of a material model depends largely on the values that the user/engineer will choose for the parameters of the model. In most cases in order to select appropriate values, calibration of the model and hence experimental results are required. Usually this sort of information is not available and therefore default values have to be used. When the law employed is sensitive to its parameters, lack of experimental results may narrow considerably its applicability. For both the Monti-Nuti and the Menegotto-Pinto models, suggested values can be obtained from various publications. A typical range for the model parameters are listed in

Table 1. Bold letters denote the values that have been found appropriate for a wide range of applications by the authors.

Table 1 Material model parameters – Range of values

	R_0	a_1	a_2	a_3	a_4	P
Men.- Pinto	20	18.5	0.05- **0.15**	0.01 – **0.025**	**2** – 7	-
Monti - Nuti	20	18.5	0.05- **0.15**	-	-	0.50 - **0.90**

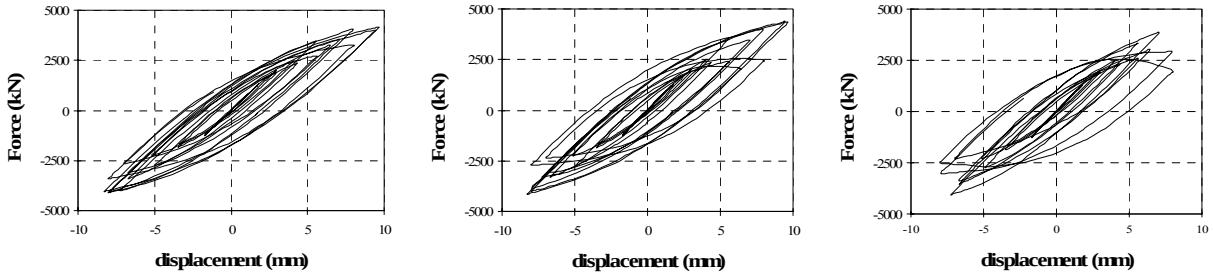

(a) (b) (c)

Figure 8. Effect of the weight parameter P on the performance of the Monti-Nuti model; (a) P=50%, (b) P=75% and (c) P=90%.

All the parameters of Table 1 have a clear physical meaning as described in the original publications. The curvature parameters R_0, a_1 and a_2 affect the shape of the hysteretic curve and hence the representation of the Bauschinger effect and the pinching of the hysteretic loops. Parameters a_3 and a_4 quantify isotropic hardening. Usually the contribution of isotropic hardening is significantly smaller than that of kinematic and hence the set of values adopted would not affect considerably the response. In Fig. (8) the parameter P is varied thus demonstrating the influence of isotropic over kinematic hardening. A simple calibration procedure for this parameter that consists of single cycle tests is suggested in the original paper of Monti and Nuti.

6 NUMERICAL STUDIES

6.1 Column under Cyclic Loading Conditions

The first case study consists of a cantilever column subjected to a displacement of constantly increasing amplitude on its top. The loading program for the specimen consisted of a displacement-controlled cyclic loading scheme, where two cycles of displacement are applied at each deformation level with 2 mm/step increments. The displacement of the tip of the column, the FE model and the properties of the column are shown in Figure 9.

The response obtained using three different reinforcing steel models is shown in Figure 10. The widely used bilinear model with kinematic hardening and the model of Menegotto and Pinto do not show degradation in the capacity of the column as opposed to the Monti-Nuti model where the envelope of the hysteretic loops shows clearly the reduction in the capacity of the column. It is also observed that, dissipation of energy and pinching of the hysteretic loops is not fully captured by the first two models.

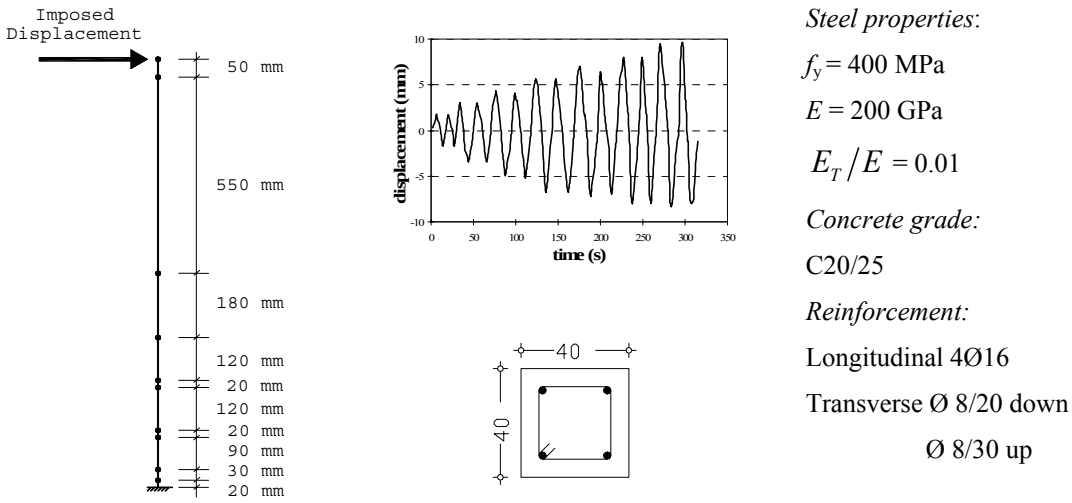

Figure 9. Geometry, FE model, loading scheme and properties of the column.

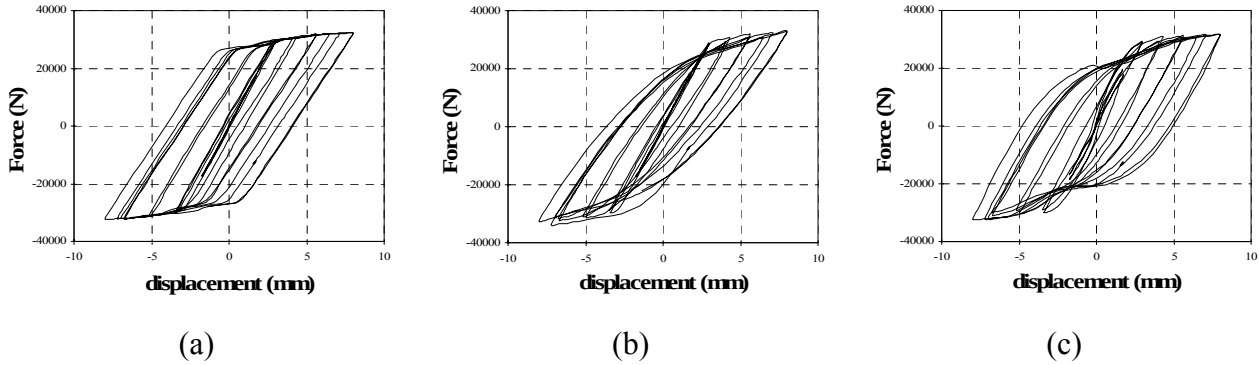

Figure 10. Response of a cantilever beam; (a) bilinear kinematic hardening (b) M-P and (c) M-N.

6.2 Wall under Dynamic Loading Conditions

This case study is part of a series of shaking table tests carried out at the Centre for Earthquake Studies and Equipment at LNEC (Lisbon, Portugal). Details concerning the project and the actual test set up are reported by Pinho *et al.* [13].

Ductility class 'L' was adopted to determine section size and longitudinal reinforcement requirements. The wall element with thickness of 200mm and its height and width are indicated in Fig. 11. Both longitudinal and shear reinforcement are also shown in Figure 11. A combination of two artificial (AR) and two natural records (NR) was applied to generate the input ground motion shown Fig. 12 [13]. The resulting ground motion guarantees that the wall will be damaged progressively. The record was split into four stages, using scaled up and scaled down accelerograms in succession, without pause, mixing both natural and artificial records. The records, in order applied, were AR(0.14), NR(0.25), NR(0.33) and AR(0.18). The second portion of the nomenclature indicates the peak ground acceleration of each record.

The transverse reinforcement used consists of ∅6/60 for the lower half and ∅6/120 for the upper half, while ∅8 bars were used for the longitudinal reinforcement. Therefore, the *L*/*D* ratios of the wall are 7.5 and 15, respectively. Thus, buckling of the longitudinal reinforcement is expected to take place and therefore considerable improvement of the results is expected when the Monti and Nuti rules are taken into consideration during analysis.

The default model parameters are used (see Table 1), while the corrective algorithm was adopted with 2.5% filtering of ε_r .

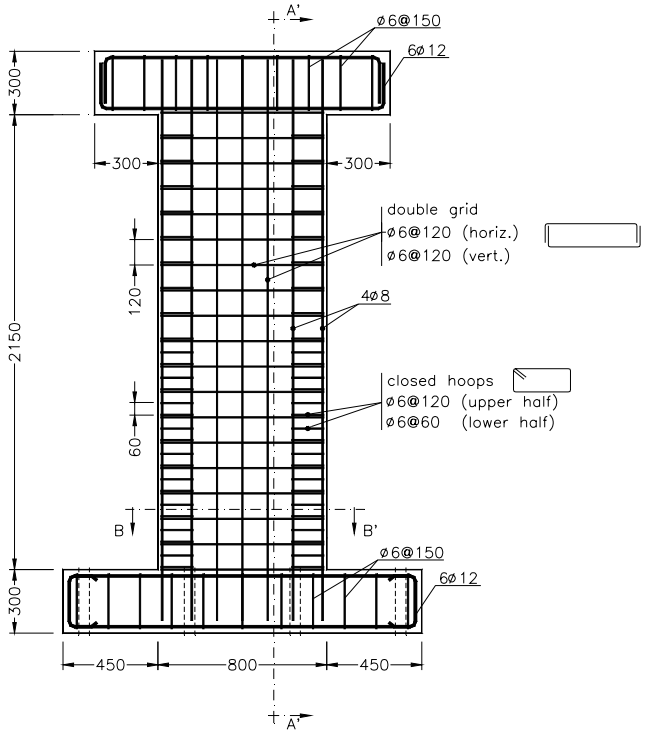

Figure 11. Dimensions and detailing of the test specimen

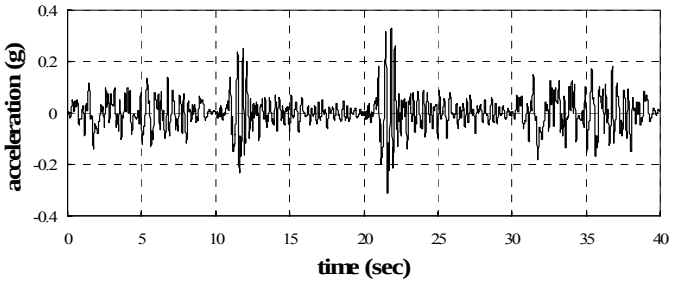

Figure 12. Acceleration ground motion record

The data acquired during the test had to be filtered so that high-frequency content, associated to parasitic vibrations in the table and electromagnetic interference, could be removed. The smooth shape of the experimental curve is therefore associated to the filtering of the records. For succinctness, stage one (time=0÷10) and three (time=20÷30) of the loading phase are presented below (Fig. 13).

Three models, the bilinear kinematic hardening, the Menegotto-Pinto and the Monti-Nuti were used for comparison. Clearly, the first fails to produce realistic hysteretic plots although the capacity and the displacements are in some cases sufficiently estimated. The Menegotto-Pinto model although it provides hysteretic curves closer to the experimental, still does not fully reproduce the experimental results. This can be attributed to some extent to the buckling of the longitudinal bars. Substantial improvement is achieved with the Monti-Nuti model. A better overall agreement is reached despite the lack of proper calibration of the model and to

some particularities present during the test set up that the FE model adopted was not able to capture.

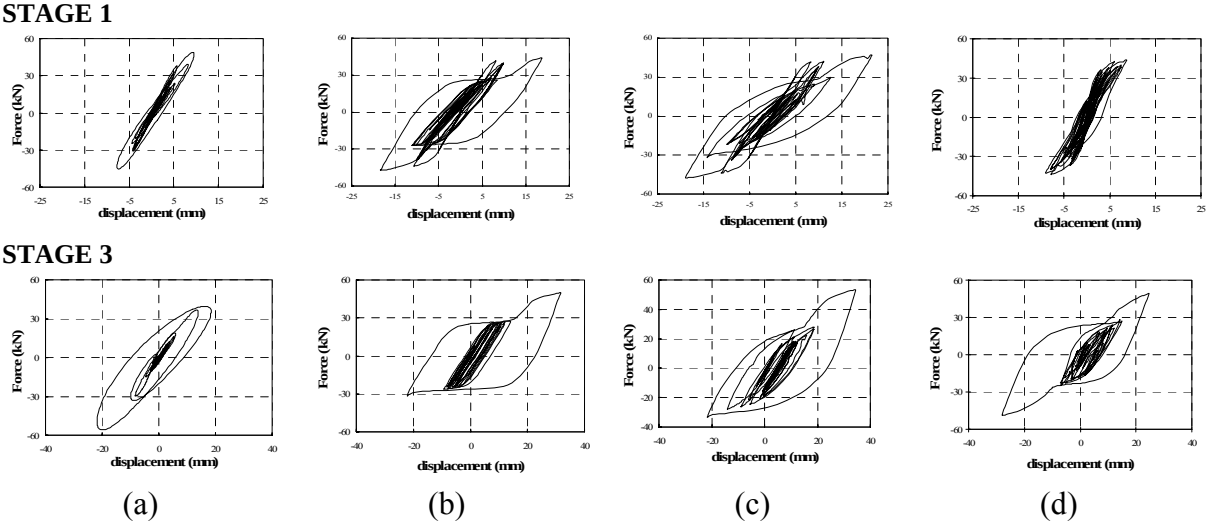

Figure 13. Wall under Dynamic Loading Conditions, the four loading stages;
(a) experimental, (b) bilinear kinematic hardening model, (c) M-P model and (d) M-N model.

7 CONCLUDING REMARKS

Buckling of the longitudinal reinforcement may affect considerably the response of RC members, especially when they are subjected to large displacements. This behaviour can be captured if the constitutive model of the reinforcement is enhanced with the experimental observations of Monti and Nuti. Monti and Nuti introduced into the Menegotto-Pinto model a set of rules for buckling of the longitudinal reinforcement. Their model, although conceptually correct, features a not necessarily unconditioned accuracy when predicting stress-strain response under a generalized load history. An additional memory rule is presented in order to tackle this shortcoming. The rule proposed is based on a relatively simple concept, and thus can also be applied in models other than that of Monti and Nuti. In the case-studies examined, improved representation of the response was obtained, though the results could still be bettered if ad-hoc model calibrations would be carried out (the latter was however outside of the scope of this work).

REFERENCES

[1] G. Monti, C. Nutti, Nonlinear behaviour of Reinforcing Bars Including Buckling, *Journal of Structural Engineering*, **118**(12), 3268-3284, 1992.

[2] M. Menegotto, P.E Pinto, Method of analysis for cyclically loaded RC plane frames including changes in geometry and nonelastic behaviour of elements under combined normal force and bending, *Proc. IABSE Symposium, Lisbon*, Portugal, 1973.

[3] F.C. Filippou, E.P. Popov, V.V. Bertero, Effects of bond deterioration on hysteretic behaviour of reinforced concrete joint, *Report No. UCB/EERC-83/19, University of California*, Berkeley, 1983.

[4] J.B. Mander, M.J.N. Priestley, R. Park, Seismic design of bridge piers, *Res. Rep. 84-2, Dept. of Civ. Engrg., Univ. of Canterbury, Christchurch*, New Zealand, 1984.

[5] S. Bae, A.M. Miesses, O. Bayrak, Inelastic Buckling of Reinforcing Bars, *Journal of Structural Engineering*, **131**(2), 314-321, 2005.

[6] E.T. Mau, M. El-Mabsout, M., Inelastic buckling of reinforcing bars, *Journal of Engineering Mechanics*, **115**(1), 1-17, 1989.

[7] E. Cosenza, A. Prota, Experimental Behaviour and Numerical Modelling of Smooth Steel Bars under Compression, *Journal of Earthquake Engineering*, **10**(3), 313-329, 2006.

[8] A. Gomes, J. Appleton, Nonlinear cyclic stress-strain relationship of reinforcing bars including buckling, *Engineering Structures*, **19**(10), 822-826, 1997.

[9] L.L Dodd, J.I. Restrepo-Posada, Model for Predicting Cyclic Behaviour of Reinforcing Steel, *Journal of Structural Engineering*, **121**(3), 433-445, 1995.

[10] T.A Balan, F.C. Filippou, E.P Popov, Hysteretic model of ordinary and high-strength reinforcing steel, *Journal of Structural Engineering*, **124**(3), 288-297, 1998.

[11] A. Attolico, S. Biondi, C. Nuti, M. Petrangeli, Influence of Buckling of Longitudinal Rebars in Finite Element Modelling of Reinforced Concrete Structures Subjected to Cyclic loading: Two Case Studies, *Proc. of Workshop on "Seismic Protection of Existing and New Construction Buildings by means of Unconventional Systems, Prin 97*, Naples, 12-13 May, 2000.

[12] M. Fragiadakis, Nonlinear Material Modelling of Reinforcement Steel Bars Under Transient Loading, *MSc Dissertation, Department of Civil Engineering, Imperial College London*, UK, 2001.

[13] R. Pinho R., A.S. Elnashai, C.T. Vaz, Experimental observations from shaking-table tests on selective techniques for repair and strengthening of RC walls, *Proc. Twelfth World Conference on Earthquake Engineering*, Auckland, New Zealand, Paper No. 2245, 2000.